# Great tsunamigenic earthquakes during the last 1000 years on the Alaska megathrust

Ian Shennan[1*], Natasha Barlow[1], Gary Carver[2], Frank Davies[1], Ed Garrett[1], Emma Hocking[3]

1 Sea Level Research Unit, Department of Geography, Durham University, Durham, DH1 3LE, UK
2 Carver Geologic Inc., Kodiak, Alaska, USA
3 Northumbria University, School of the Built and Natural Environment, Ellison Building, Newcastle upon Tyne, NE1 8ST, UK
* Corresponding author ian.shennan@durham.ac.uk

## ABSTRACT

**Large to great earthquakes and related tsunamis generated on the Alaska megathrust produce major hazards for both the area of rupture and heavily populated coastlines around much of the Pacific Ocean. Recent modelling studies suggest that single segment ruptures, as well as multi-segment 1964-type ruptures, can produce great earthquakes, >M8, and significant hazards in both the near-field and to distant locations through the generation of tsunamis. We present new paleoseismological data from Kodiak Island and a new analysis of radiocarbon data based on Bayesian age modelling to combine our observations with previous geological, historical and archaeological investigations. We suggest that in addition to multi-segment ruptures in 1964 and AD 1020-1150 (95% age estimate), a single segment rupture occurred in 1788, with coseismic land surface deformation across Kodiak Island and a tsunami that is recorded in historical documents and in sediment sequences, and another, similar rupture of the same Kodiak segment AD 1440-1620. These indicate shorter intervals between ruptures of the Kodiak segment than previously assumed, and more frequent than for the Prince William Sound segment.**

## INTRODUCTION AND AIMS

The eastern segments of the Alaska-Aleutian megathrust are source areas of significant seismic hazards, generating great, >M8.0, earthquakes and tsunamis that may propagate across much of the northeast Pacific Ocean (Kirby et al., 2013; Ryan et al., 2012; SAFFR, 2013). Source areas from the Alaska megathrust, structurally different from the island arc Aleutian megathrust (von Huene et al., 2012), include the Prince William Sound and Kodiak segments, which ruptured together during the M9.2 great Alaska earthquake of 1964, and the Semidi segment, that ruptured in 1938, with a M8.3 earthquake (Carver and Plafker, 2008; Freymueller et al., 2008). Recent modelling of tsunami impacts along the coast of California and Hawaii highlights the hazard that ruptures of even single segments of the Alaska megathrust pose to Pacific coasts but note the lack of the geological evidence for the ages, recurrence and rupture dimensions of previous events (Butler, 2012; Kirby et al., 2013; SAFFR, 2013). Paleoseismic evidence from coastal sediments currently provide a good record of the recurrence of these large events only for the Prince William Sound segment, with widespread evidence of seven great earthquakes in the last 4000 years (Shennan et al., 2014) and ten in the last 6000 years (Carver and Plafker, 2008). Less is known about the recurrence of great earthquakes in the Kodiak and Semidi segments. West of this, in the Shumagain Gap, aseismic slip dominates at least the last 3400 years (Witter et al., 2014). Here we present new field evidence of recent ruptures from three coastal marshes on Kodiak Island. We provide a new synthesis and temporal model that combines our new findings with those of previous paleoseismic studies across the Kodiak archipelago and historical records. We aim to explain variations in the spatial pattern of coseismic surface deformation between sites during late Holocene earthquakes and relate these to ruptures of different segments of the megathrust.

The 1964 Alaska earthquake ruptured ~950 km of the megathrust, involving the Kodiak and Prince William Sound segments (Carver and Plafker, 2008), and produced coseismic uplift in a largely offshore area and a zone of subsidence largely onshore and along the coast to the north and northwest (Figure 1). Changes in sediment lithology and biostratigraphy of coastal marshes can register coseismic vertical land motions, providing records of 1964 and previous great earthquakes. Correlations between sites across the Prince William Sound segment estimate the age of the penultimate great earthquake as AD 1020-1150 (Shennan et al., 2014). In contrast, geological evidence exists to suggest that the penultimate great earthquake in the Kodiak segment was more recent, AD 1417-1477 (Carver and Plafker, 2008; Gilpin, 1995); and limited historical accounts of an event in the Semidi segment in 1788 (Boyd et al., 1988; Briggs et al., 2014; Soloviev, 1990; Sykes et al., 1980).

**RESULTS**

Coastal marshes at all three field sites for our new investigations on Kodiak Island underwent 1.2-1.5 ±0.3 m coseismic subsidence during the 1964 earthquake (Plafker, 1969; Plafker and Kachadoorian, 1966) and we use stratigraphic evidence to identify previous episodes of marsh submergence. Five critical criteria help determine a coseismic record and discriminate from non-seismic processes that might cause rapid marsh submergence; 1 - lateral extent of peat-mud couplets with sharp contacts; 2 - suddenness of subsidence; 3 - amount of vertical motion; 4 - presence of tsunami sediments and, 5 - synchroneity with other sites (Nelson et al., 1996). The distinctive Katmai tephra, from AD 1912, is a critical chronostratigraphic marker at all our sites on Kodiak and adjacent islands. We reconstruct marsh stratigraphy using cleaned outcrops and series of hand-drilled cores (Figure 1). In some areas a peat-mud couplet occurs above the Katmai tephra; this is the sedimentary record of marsh submergence in 1964. In the sediments beneath the Katmai tephra we could trace one major peat-mud couplet, with a sharp contact, across 100s of metres at two sites, Middle Bay and Kalsin Bay, and across ~100 m at Anton Larson Bay. It is often overlain by a silt/sand layer, capped by organic silt that increases in organic content up-core. In some cores the organic silt grades upward into herbaceous peat. We found numerous other minerogenic units either within peat units or above them, with sharp contacts; but we could not trace them over such long distances and at present we do not have sufficient evidence to suggest additional episodes of coseismic submergence. We use sediment lithology and diatom data to identify tsunami sediments and relative land-level change across each peat-mud couplet (Figure 2a). Transfer function models, derived from the modern relationships between diatom species and tidal range and applied to fossil diatom assemblages preserved in Holocene sediments, allow us to quantify elevation change through sediment profiles (Supplementary Information files), excluding the data from any tsunami layer as the diatoms will come from mixed sources. Reconstructions indicate subsidence at all three sites (Figure 2b) on the order of a few decimetres, substantially less deformation than in 1964.

In order to determine the chronology at each site and to correlate between sites we use the OxCal Bayesian modelling approach (Bronk Ramsey, 2009; Lienkaemper and Bronk Ramsey, 2009) to determine the best-fit age of the penultimate earthquake, i.e. pre-1964 and stratigraphically the first below the Katmai tephra. It allows us to combine the radiocarbon ages on the earthquake horizon from sites across the Kodiak segment (Supplementary Information files), whether the site records coseismic uplift or coseismic subsidence. This approach assumes the dated indicators of uplift or subsidence are either minimum or maximum ages on the earthquake horizon. For coseismic subsidence, maximum ages come from a peat contact below an intertidal mud unit and minimum ages from samples within the mud unit. For coseismic uplift, maximum ages come from the top part of intertidal mud below peat, and minimum ages from the peat. The Bayesian model seeks to estimate the age of each earthquake that is bracketed by dated samples assuming no knowledge of sedimentation rate pre- or post- earthquake. Samples are grouped into "phases", where one phase is all the samples giving a minimum age on an earthquake, and another phase will be all the maximum ages for the earthquake (Lienkaemper and Bronk Ramsey, 2009; Shennan et al., 2014). There is no chronological ordering within a phase, but the stratigraphic ordering of phases, the earthquake horizon and the Katmai tephra are powerful constraints on the model.

For our first chronological model we test the hypothesis of one single segment rupture of the Kodiak segment ~AD 1417-1477 (Carver and Plafker, 2008; Gilpin, 1995), between the multi-segment ruptures in 1964 and ~AD 1020-1150, when the Prince William Sound and Kodiak segments ruptured together (Carver and Plafker, 2008; Shennan et al., 2014). We include all data from the whole Kodiak segment with conventional radiocarbon ages younger than AD1000 and find there is no numerical convergence in the model and therefore no acceptable fit. Maximum and minimum ages that bracket the submergence event horizon at four sites in northwest Kodiak and ages from one site bracketing uplift on Sitkalidak Island are significantly older than those from four sites in SE Kodiak (Supplementary Information). These younger samples date tsunami inundation of middens and houses at Settlement Point on Afognak River (Carver and Plafker, 2008; Hutchinson and Crowell, 2007) and the episode of marsh submergence we record at Middle Bay, Kalsin Bay and Anton Larson Bay.

Therefore we separate the samples into two geographical sets: an "outer Kodiak" group comprising the northwest Kodiak and Sitkalidak Island sites, and the four sites clustered in SE Kodiak. The outer Kodiak model estimates the age of the event to AD 1440-1620 (Figure 2c), younger than the previous estimate (Carver and Plafker, 2008), AD 1417-1477, that was based data from across all of Kodiak and adjacent islands and a different method for estimating the event age. The SE Kodiak model results (Figure 2b) show two important points. First, the incompatibility with an event age comparable to that from the outer Kodiak model; second the modelled age AD 1700-1912, that coincides with the well-documented radiocarbon plateau from ~AD 1700 to modern. This always provides a challenge to improving age estimates of events in this period without other lines of evidence. In this region, historical accounts from early Russian trading posts in SW Kodiak and along the Alaska Peninsula describe an earthquake and tsunami on 22 July 1788, followed by many aftershocks, and a second tsunami on 7 August 1788 (Davies et al., 1981; SAFFR, 2013; Soloviev, 1990). The original sources and secondary accounts leave room for quite different interpretations regarding sources and timings of events (Boyd et al., 1988; Briggs et al., 2014; Davies et al., 1981; SAFFR, 2013; Soloviev, 1990; Sykes et al., 1980). The least contentious is the description of intense ground shaking, followed by a tsunami and net submergence at Three Saints Harbor, on the south coast of Kodiak Island immediately west of Sitkalidak Island. Much more contentious are the interpretations of the evidence for whether there were one or two tsunami on the islands in the Semidi segment and the Alaska Peninsula, whether the evidence of tsunamis and ground shaking without descriptions of land uplift or subsidence are sufficient to determine rupture extent, or whether there were two earthquakes in 1788 (Briggs et al., 2014). Opinions range from one great earthquake on 22 July from a rupture that extended from southwest Kodiak and westwards for ~500 km, equivalent to the Semidi segment, to a submarine slump causing the August 7 tsunami, as there are no accounts of ground shaking for that day (Kirby et al., 2013).

## DISCUSSION AND CONCLUSIONS

We suggest that the SE Kodiak data provide the first evidence to support a hypothesis of an earthquake in 1788, probably July 22nd, causing net subsidence across Kodiak Island from at least Three Saints Harbour to Settlement Point (Figure 3b) and uplift in Sitkinak (Briggs et al., 2014). We see tsunami sediments and net subsidence at Kalsin Bay and Settlement Point, and net subsidence but no tsunami at Middle Bay and Anton Larson Bay. Although the studies that provide the evidence of coseismic subsidence AD 1440-1620 along the northwest coast of Kodiak do not date any younger sequences (Gilpin, 1995) we note that stratigraphic sections in two areas show a younger event (Figure 3b). Subsidence within the Kodiak segment followed a similar spatial pattern to that observed in 1964 but with less vertical motion, ~0.2-0.3 m (Figure 2b) compared to 1.2-1.5±0.3 m at the same sites. We also conclude that the earlier event, AD 1440-1620, is evidence of another rupture of the Kodiak segment (Figure 3c). At our new sites in SE Kodiak we find no laterally continuous record of submergence; only a single outcrop at Middle Bay shows a possible tsunami sediment and possible subsidence, within the elevation uncertainties (Figure 2a). Lesser deformation throughout or a slight change in the spatial pattern of deformation would place our sites at the limit of detecting submergence or close to the zero contour respectively. With the data currently available we conclude there is insufficient evidence to determine minor differences in rupture area and propose that both the AD 1440-1620 and 1788 events are earthquakes generated by slip on the Kodiak segment of the megathrust.

In 1964 the asperity in this segment was opposite the Kodiak seamount, part of the Kodiak-Bowie seamount chain (Figure 3a). The patterns of uplift and subsidence inferred for AD 1440-1620 and 1788 (Figure 3b,c) suggest a similar asperity, with the rupture extending beyond the subducting seamounts along the 58° Fracture Zone, but not past the lower plate features that separate the 1964 Kodiak and Prince William Sound segments (von Huene et al., 2012).

Variations in the relief and sediment thickness at the subducting plate interface means that the seismic cycle of features such as the Kodiak-Bowie and 58° Fracture Zone seamount chains of the Kodiak segment can be in or out of phase with the surrounding plate interface cycle (von Huene et al., 2012). It now seems that the Kodiak segment generated great earthquakes on at least 4 occasions since AD

1020-1150 compared to two ruptures of Prince William Sound segment. Although the evidence in Kodiak is sparse for older events (Carver and Plafker, 2008; Gilpin, 1995), current thought is that in AD 1020-1150 the Kodiak, Prince William Sound and probably the Yakataga segments ruptured together (Shennan et al., 2014; Shennan et al., 2009). In 1964 the Kodiak segment ruptured with the Prince William Sound segment. In 1788 it was at a minimum a single segment rupture. Historical accounts of a tsunami may indicate a larger rupture (Davies et al., 1981; Soloviev, 1990), including part or the entire Semidi segment but that remains open to debate (Briggs et al., 2014; Witter et al., 2014). The AD 1440-1620 earthquake and tsunami is only recorded, so far, in the Kodiak segment. In terms of seismic hazard analysis, evidence for older events in the Kodiak segment will require detailed stratigraphic approaches to separate potentially closely spaced events but the latest three, 1964, 1788 and AD 1440-1620, indicate a shorter interval between great earthquakes than previously assumed.

## References


Boyd, T.M., Taber, J.J., Lerner-Lam, A.L., and Beavan, J., 1988, Seismic rupture and arc segmentation within the Shumagin Islands Seismic Gap, Alaska: Geophysical Research Letters, v. 15, p. 201-204.

Briggs, R.W., Engelhart, S.E., Nelson, A.R., Dura, T., Kemp, A.C., Haeussler, P.J., Corbett, D.R., Angster, S.J., and Bradley, L.-A., 2014, Uplift and subsidence reveal a nonpersistent megathrust rupture boundary (Sitkinak Island, Alaska): Geophysical Research Letters, p. 2014GL059380.

Bronk Ramsey, C., 2009, Bayesian analysis of radiocarbon dates: Radiocarbon, v. 51, p. 337-360.

Butler, R., 2012, Re-examination of the Potential for Great Earthquakes along the Aleutian Island Arc with Implications for Tsunamis in Hawaii: Seismological Research Letters, v. 83, p. 29-38.

Carver, G., and Plafker, G., 2008, Paleoseismicity and Neotectonics of the Aleutian Subduction Zone - An Overview, *in* Freymueller, J.T., Haeussler, P.J., Wesson, R., and Ekstrom, G., eds., Active tectonics and seismic potential of Alaska: Geophysical Monograph Series: Washington, American Geophysical Union, p. 43-63.

Davies, J., Sykes, L., House, L., and Jacob, K., 1981, Shumagin Seismic Gap, Alaska Peninsula: History of great earthquakes, tectonic setting, and evidence for high seismic potential: Journal of Geophysical Research: Solid Earth, v. 86, p. 3821-3855.

Freymueller, J.T., Woodard, H., Cohen, S.C., Cross, R., Elliott, J., Larsen, C.F., Hreinsd, oacute, ttir, S., and Zweck, C., 2008, Active deformation processes in Alaska, based on 15 years of GPS measurements, *in* Freymueller, J.T., Haeussler, P.J., Wesson, R., and Ekström, G., eds., Active Tectonics and Seismic Potential of Alaska, Volume 179: Geophysical Monograph Series: Washington, DC, AGU, p. 1-42.

Gilpin, L.M., 1995, Holocene paleoseismicity and coastal tectonics of the Kodiak Islands, Alaska: Santa Cruz, University of California Santa Cruz.

Hutchinson, I., and Crowell, A.L., 2007, Recurrence and Extent of Great Earthquakes in Southern Alaska During the Late Holocene from an Analysis of the Radiocarbon Record of Land-Level Change and Village Abandonment: Radiocarbon, v. 49, p. 1323-1385.

Kirby, S., Scholl, D., W., von Huene, R., and Wells, R., E., 2013, Alaska earthquake source for the SAFRR tsunami Scenario. U.S. Geological Survey Open-File Report 2013-1170-B, : US Geological Survey Open File Report 2012-1170-B http://pubs.usgs.gov/of/2013/1170/d/. , p. 40.

Lienkaemper, J.J., and Bronk Ramsey, C., 2009, OxCal: Versatile tool for developing paleoearthquake chronolgies - A primer: Seismological Research Letters, v. 80, p. 431-434.

Nelson, A.R., Shennan, I., and Long, A.J., 1996, Identifying coseismic subsidence in tidal-wetland stratigraphic sequences at the Cascadia subduction zone of western North America: Journal of Geophysical Research, v. 101, p. 6115-6135.

Plafker, G., 1969, Tectonics of the March 27, 1964, Alaska earthquake: U.S. Geological Survey Professional Paper, v. 543-I, p. 74.

Plafker, G., and Kachadoorian, R., 1966, Geologic effects of the March 1964 earthquake and associated seismic sea waves on Kodiak and nearby islands, Alaska: U.S. Geological Survey Professional Paper, v. 543-D, p. 46.

Ryan, H., F., von Huene, R., Wells, R., E., Scholl, D., W., Kirby, S., and Draut, A., E. , 2012, History of earthquakes and tsunamis along the eastern Aleutian-Alaska megathrust, with implications for tsunami hazards in the California continental borderland: U.S. Geological Survey Professional Paper, v. 1795-A, p. 31.

SAFFR, 2013, (Science Application for Risk Reduction) Tsunami Modeling Working Group: Modeling for the SAFRR Tsunami Scenario-Generation, propagation, inundation, and currents in ports and harbors. U.S. Geological Survey Open-File Report 2013-1170-D US Geological Survey Open File Report 2012-1170 http://pubs.usgs.gov/of/2013/1170/d/. , p. 136.

Shennan, I., Bruhn, R., Barlow, N., Good, K., and Hocking, E., 2014, Late Holocene great earthquakes in the eastern part of the Aleutian megathrust: Quaternary Science Reviews, v. 84, p. 86-97.

Shennan, I., Bruhn, R., and Plafker, G., 2009, Multi-segment earthquakes and tsunami potential of the Aleutian megathrust: Quaternary Science Reviews, v. 28, p. 7-13.

Soloviev, S.L., 1990, Sanak-Kodiak tsunami of 1788: Science of tsunami hazards, v. 8, p. 34-30.

Sykes, L.R., Kisslinger, J.B., House, L., Davies, J.N., and Jacob, K.H., 1980, Rupture Zones of Great Earthquakes in the Alaska-Aleutian Arc, 1784 to 1980: Science, v. 210, p. 1343-1345.

von Huene, R., Miller, J.J., and Weinrebe, W., 2012, Subducting plate geology in three great earthquake ruptures of the western Alaska margin, Kodiak to Unimak: Geosphere, v. 8, p. 628-644.

Witter, R.C., Briggs, R.W., Engelhart, S.E., Gelfenbaum, G., Koehler, R.D., and Barnhart, W.D., 2014, Little late Holocene strain accumulation and release on the Aleutian megathrust below the Shumagin Islands, Alaska: Geophysical Research Letters, p. 2014GL059393.

## Acknowledgements

This work is supported by the U.S. Geological Survey earthquake hazards project awards G10AP00075 and GA12AP20084 (The views and conclusions contained in this document are those of the authors and should not be interpreted as necessarily representing the official policies, either expressed or implied, of the U.S. Government). Roland von Heune, Rich Briggs and Dave Scholl for helpful reviews.

## Supplementary Information Files

1. Table of radiocarbon data used for age modelling
2. Oxcal model outputs
3. Diatom diagrams to illustrate the data used in transfer function reconstructions of elevation

4. Transfer function estimated elevation change across earthquake horizons
5. Stratigraphic sections and radiocarbon ages from Kalsin Bay

**Figure Legends**

Figure 1: a) Kodiak site locations and rupture zones on the Alaska megathrust: co-rupture of the Kodiak segment and the Prince William Sound segment in 1964; the Semidi segment in 1938. b) Middle Bay site, core locations, with outcrops at 1,2,3,4, and 15. c) stratigraphic section at Middle Bay with radiocarbon dated samples shown as 95% calibrated age ranges AD, with upper limit defined by the Katmai tephra age where relevant.

Figure 2: a) stratigraphy of the outcrop at Middle Bay, location 1, with summary diatom classes and reconstruction of relative sea level (RSL). RSL rise at 82 cm depth interpreted as coseismic submergence in 1788. Sand layer at 114-118 cm and associated RSL change discussed in text. b) estimates of coseismic deformation in 1788 from sediment cores at Anton Larson Bay, Middle Bay and Kalsin Bay, with 95% ranges. c) Documented ages, 1788 and 1964 and 95% probability density functions of modelled ages for earthquakes in the last 1000 years. Details of age model in supplementary files.

Figure 3: summary of coseismic land motions, inferred rupture zones and selected features of subducting lower plate relief that may influence earthquake rupture (von Huene et al., 2012). a) 1964 (observations from Plafker, 1969). b) 1788 and c) AD 1440-1620: relative ground motions inferred from sediment stratigraphy and microfossil analyses where present (figure 2b and from Sitkinak, Briggs et al. 2014). Extent of Kodiak segment from von Heune et al. (2012); dashed line for the 1788 rupture indicates alternative interpretation of historical documentary evidence.

Figure 1

Click here to download high resolution image

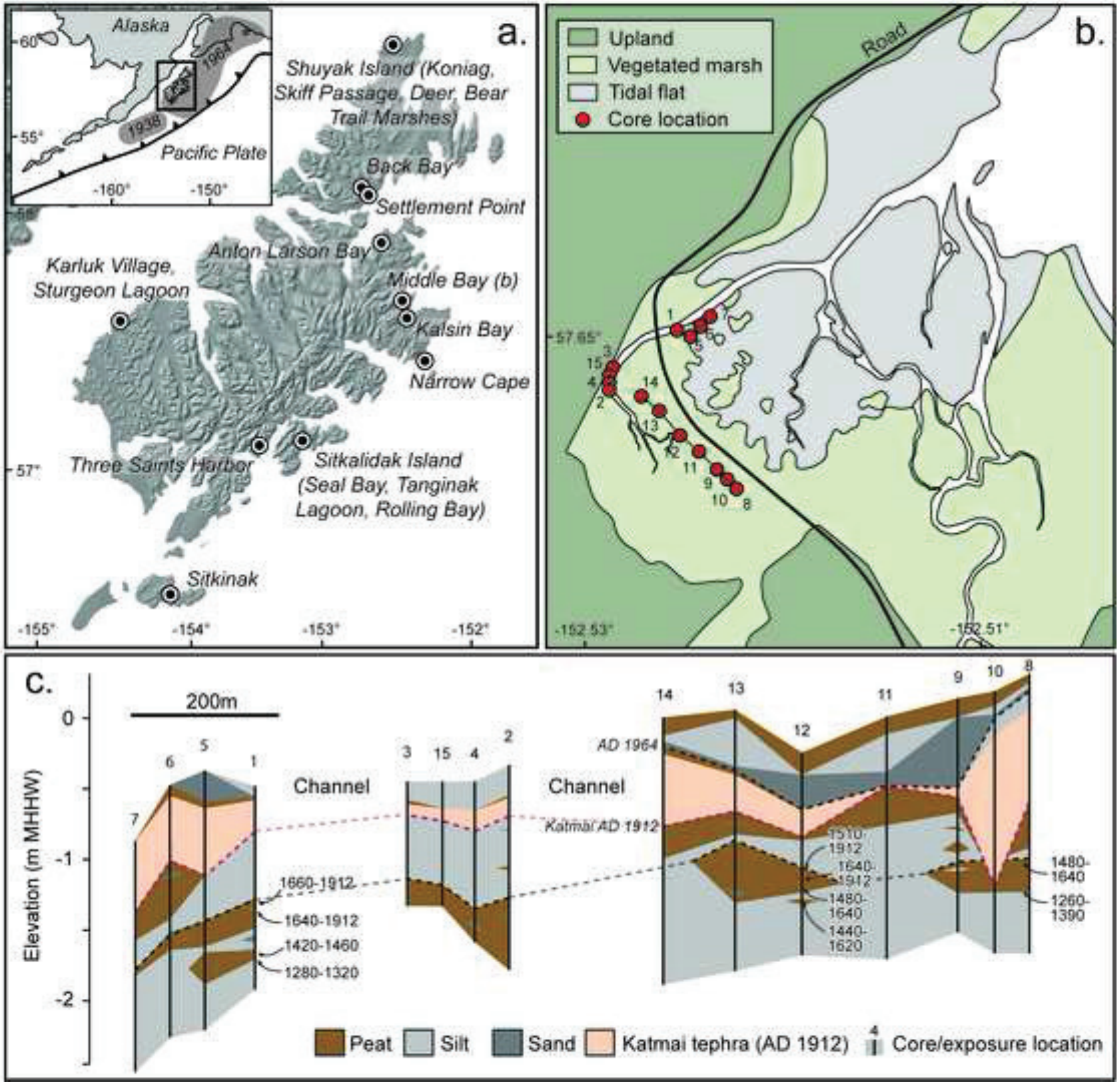

Figure 2
Click here to download high resolution image

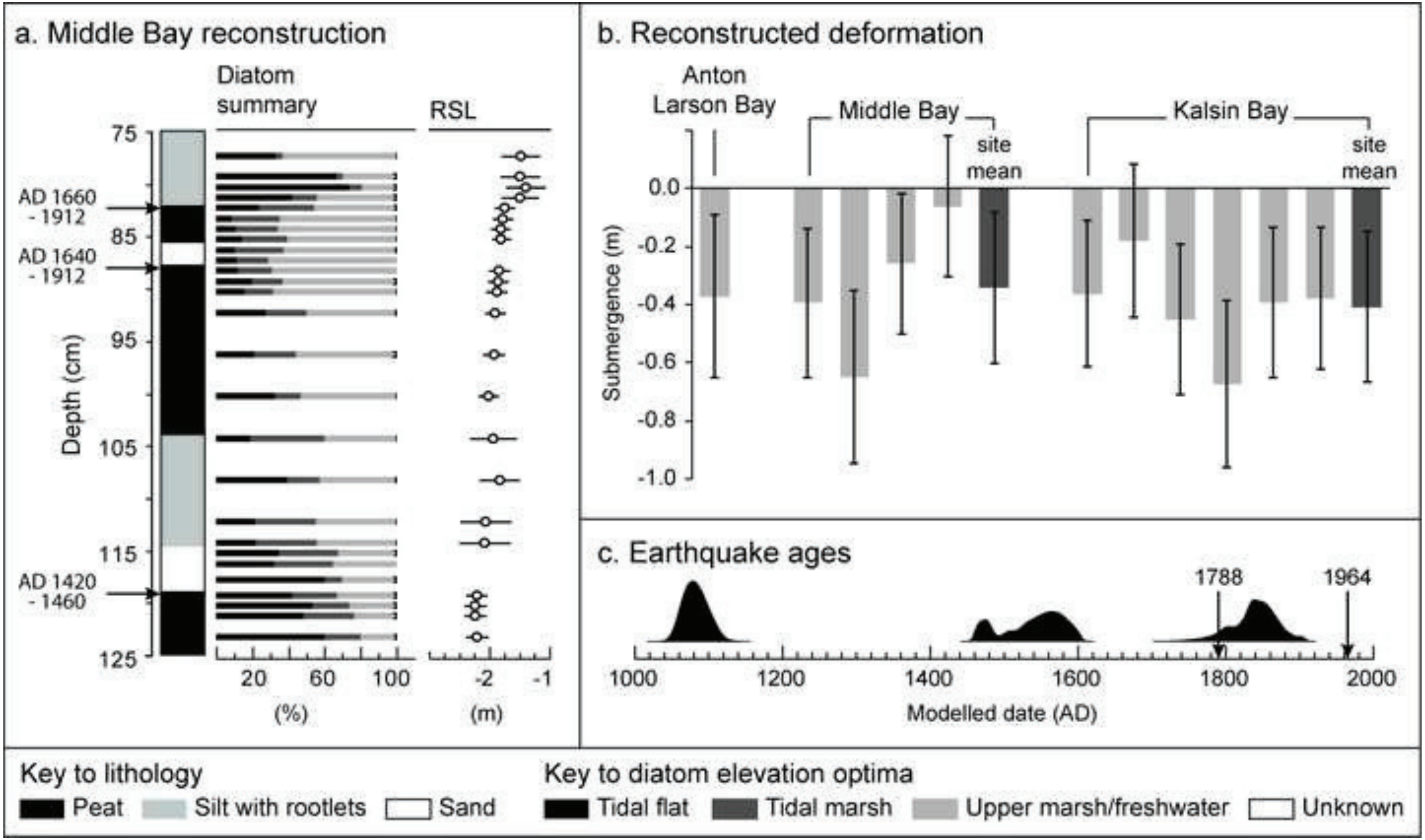

Figure 3
Click here to download high resolution image

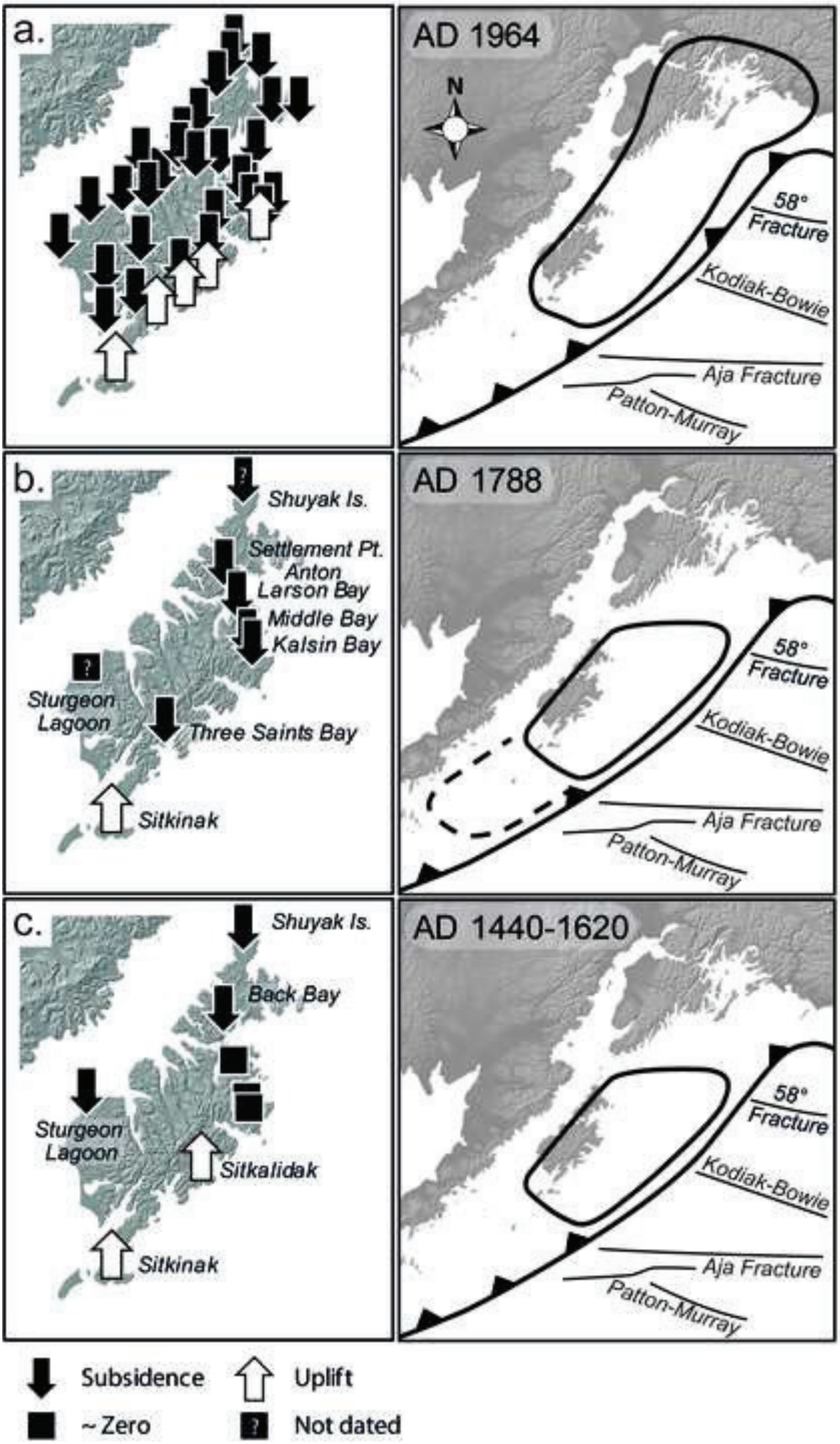

Supplementary Information: Radiocarbon ages constraining earthquake event horizons

Page 1 – site locations
Page 2 – radiocarbon ages and stratigraphic context

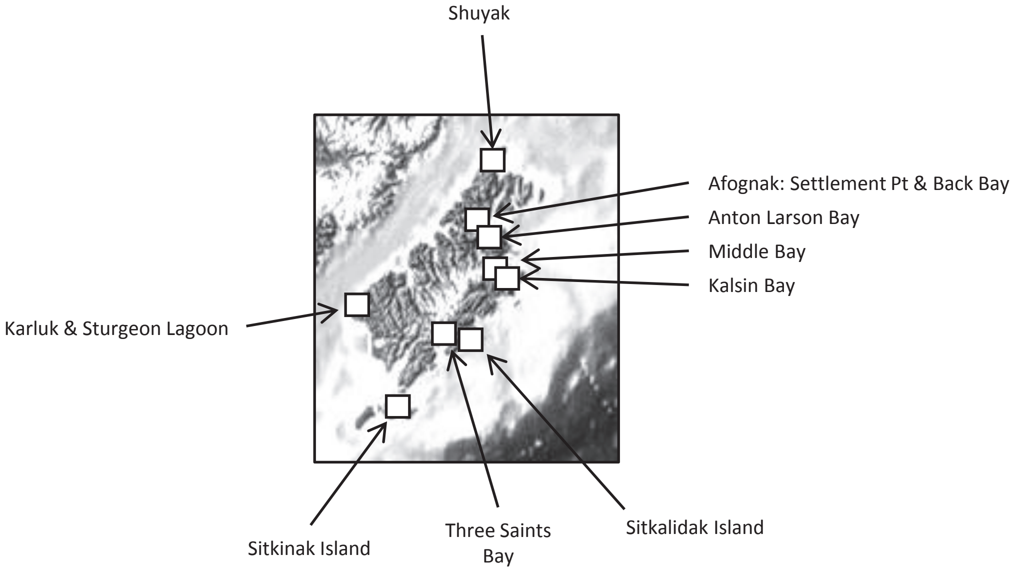

Supplementary Information: Radiocarbon ages constraining earthquake event horizons

Sources: 1: Carver & Plafker 2008

2: Gilpin 1995

3: This paper

| Laboratory Code | 14C BP | SD | Site | Code in original source | Context | Maximum or minimum constraint on event | Source |
|---|---|---|---|---|---|---|---|
| Outer Kodiak locations | | | | | | | |
| QL-4746 | 770 | 25 | Sitkalidak - Rolling Bay | SDI-92-RB-1-83-4 | Peat below event horizon | Max | 1, 2 |
| Beta-???? | 740 | 80 | Karluk Village | Karluk-Archeo | Charcoal below event horizon | Max | 1, 2 |
| QL-4671 | 625 | 30 | Sitkalidak - Seal Bay | SDI-92-2-1-73 | Triglochin peat below event horizon | Max | 1, 2 |
| QL-4743 | 615 | 15 | Karluk Village | Karluk-Archeo | Wood below event horizon | Max | 1, 2 |
| QL-4597 | 494 | 23 | Shuyak - Deer Marsh | SI-A-5-2.80 | Triglochin peat below event horizon | Max | 1, 2 |
| QL-4750 | 490 | 20 | Shuyak - Bear Trail Marsh | SI-93-A-7-1-46 | Peat below event horizon | Max | 1, 2 |
| QL-4667 | 483 | 26 | Afognak - Back Bay | AI-A-1-51 | Sphagnum peat below event horizon | Max | 1, 2 |
| QL-4592 | 443 | 14 | Shuyak - Skiff Passage Marsh | SI-A-4-2.15 | Sphagnum peat below event horizon | Max | 1, 2 |
| QL-4590 | 330 | 30 | Shuyak - Koniag Marsh | SI-A-2-1.55 | Sphagnum peat below event horizon | Max | 1, 2 |
| QL-4742 | 330 | 25 | Shuyak - Skiff Passage Marsh | SI-A-4-70-72 | Peat below event horizon | Max | 1, 2 |
| QL-4669 | 330 | 30 | Sturgeon Lagoon | KI-KK-A-2-61 | Sphagnum peat below event horizon | Max | 1, 2 |
| Earthquake age to model | | | | | | | |
| QL-4745 | 610 | 70 | Sitkalidak - Seal Bay | SDI-92-2-1-72 | Peat above event horizon | Min | 1, 2 |
| Beta-48802 | 580 | 60 | Sturgeon Lagoon | KI-KK-A-2-59 | Triglochin peat above event horizon | Min | 1, 2 |
| Beta-48806 | 460 | 50 | Shuyak - Deer Marsh | SI-A-5-1.9 | Triglochin peat above event horizon | Min | 1, 2 |
| QL-4596 | 447 | 30 | Shuyak - Deer Marsh | SI-A-5-2.75 | Triglochin peat above event horizon | Min | 1, 2 |
| QL-4595 | 416 | 14 | Shuyak - Deer Marsh | SI-A-5-1.9 | Triglochin peat above event horizon | Min | 1, 2 |
| Beta-48804 | 380 | 60 | Afognak - Back Bay | AI-A-1-49 | Triglochin peat above event horizon | Min | 1, 2 |
| QL-4589 | 310 | 30 | Shuyak - Koniag Marsh | SI-A-2-1.50 | Triglochin peat above event horizon | Min | 1, 2 |
| QL-4741 | 260 | 20 | Shuyak - Skiff Passage Marsh | SI-A-4-66-68 | Triglochin peat above event horizon | Min | 1, 2 |
| QL-4749 | 180 | 25 | Shuyak - Bear Trail Marsh | SI-A-7-1-35 | Peat above event horizon | Min | 1, 2 |
| Katmai tephra AD 1912 | | | | | | | |
| | | | | | | | |
| SE Kodiak locations | | | | | | | |
| AA357775 | 770 | 30 | Kalsin Bay | KB13/27 109cm | Base of organic sequence | Max | 3 |
| AA357772 | 730 | 30 | Kalsin Bay | KB13/5 110cm | Within silt-peat below event horizon | Max | 3 |
| QL-4587 | 710 | 30 | Middle Bay | KI-SC-1-150 | Triglochin peat below event horizon | Max | 1,2 |
| AA299879 | 700 | 30 | Middle Bay | MB10/8 153.5cm | Base of peat below event horizon | Max | 3 |
| AA356279 | 670 | 30 | Middle Bay | MB13/1 143cm | Base of organic sequence | Max | 3 |
| Beta-101551 | 620 | 50 | Afognak - Settlement Point | House 1 hearth | Charcoal below event horizon | Max | 1 |
| AA356272 | 590 | 30 | Kalsin Bay | KB13/29 69.5cm | Top of peat below event horizon | Max | 3 |
| Beta-118300 | 570 | 60 | Afognak - Settlement Point | House 2 hearth | Charcoal below event horizon | Max | 1 |
| QL-4586 | 500 | 20 | Kalsin Bay | KI-KL-3A-4.8 | Sphagnum peat below event horizon | Max | 1,2 |
| AA357774 | 450 | 30 | Kalsin Bay | KB13/27 89cm | Top of peat below event horizon | Max | 3 |
| AA357411 | 450 | 30 | Middle Bay | MB13/1 119cm | Within peat below event horizon | Max | 3 |
| Beta-114204 | 450 | 50 | Afognak - Settlement Point | House 7 floor | Charcoal below event horizon | Max | 1 |
| Beta-114202 | 440 | 60 | Afognak - Settlement Point | House 5 floor | Charcoal below event horizon | Max | 1 |
| Beta-101912 | 440 | 50 | Afognak - Settlement Point | Midden bottom L2 | Charcoal below event horizon | Max | 1 |
| AA295551 | 420 | 30 | Middle Bay | MB10/12 93cm | Base of peat below event horizon | Max | 3 |
| AA287207 | 410 | 40 | Middle Bay | MB10/5C 107cm | Top of peat below event horizon | Max | 3 |
| Beta-101913 | 390 | 50 | Afognak - Settlement Point | Midden | Charcoal below event horizon | Max | 1 |
| AA287205 | 370 | 40 | Anton Larson Bay | ALB10/4 78.5cm | Top of peat below event horizon | Max | 3 |
| Beta-114096 | 370 | 80 | Afognak - Settlement Point | Midden L1 | Settlement Point Charcoal K-Max | Max | 1 |
| Beta-114097 | 350 | 70 | Afognak - Settlement Point | House 3 floor | Settlement Point Charcoal K-Max | Max | 1 |
| Beta-114098 | 340 | 60 | Afognak - Settlement Point | Midden L2G | Settlement Point Charcoal K-Max | Max | 1 |
| AA287208 | 330 | 40 | Middle Bay | MB10/5C 124cm | Within peat below event horizon | Max | 3 |
| AA299878 | 330 | 30 | Middle Bay | MB10/8 130cm | Top of peat below event horizon | Max | 3 |
| Beta-114203 | 330 | 60 | Afognak - Settlement Point | House 4 floor | Settlement Point Charcoal K-Max | Max | 1 |
| AA295550 | 320 | 30 | Middle Bay | MB10/12 90cm | Peat below event horizon | Max | 3 |
| Beta-101552 | 300 | 50 | Afognak - Settlement Point | House 1 floor | Charcoal below event horizon | Max | 1 |
| Beta-114205 | 300 | 50 | Afognak - Settlement Point | House 6 floor | Charcoal below event horizon | Max | 1 |
| AA295548 | 270 | 30 | Middle Bay | MB10/12 70cm | Top of peat below event horizon | Max | 3 |
| AA357821 | 220 | 30 | Middle Bay | MB13/1 88cm | Peat below event horizon | Max | 3 |
| AA295549 | 210 | 30 | Middle Bay | MB10/12 83cm | Peat below event horizon | Max | 3 |
| AA357408 | 200 | 30 | Kalsin Bay | KB13/5 116cm | Peat below event horizon | Max | 3 |
| AA356276 | 160 | 30 | Middle Bay | MB13/1 82cm | Top of peat below event horizon | Max | 3 |
| AA357409 | 150 | 30 | Kalsin Bay | KB13/17 101cm | Top of peat below event horizon | Max | 3 |
| AA356271 | 90 | 30 | Kalsin Bay | KB13/22 72cm | Top of peat below event horizon | Max | 3 |
| AA356280 | 40 | 30 | Middle Bay | MB13/4 91cm | Top of peat below event horizon | Max | 3 |
| AA356266 | 10 | 30 | Kalsin Bay | KB13/5 92cm | Top of peat below event horizon | Max | 3 |
| Earthquake age to model | | | | | | | |
| AA357771 | 130 | 40 | Kalsin Bay | KB13/5 77cm | Base of peat below Katmai tephra | Min | 3 |
| Beta-48801 | 90 | 60 | Kalsin Bay | KI-KL-3B-4.88 | Wood above event horizon | Min | 1 |
| Katmai tephra AD 1912 | | | | | | | |

Supplementary Information: Age model outputs

Software: OxCal v4.2.3 https://c14.arch.ox.ac.uk Bronk Ramsey (2013)

Model 1: All data from Kodiak Region (details of all samples in Supplementary Information file "Radiocarbon Ages"); assume that the earthquake horizon at each site is the same event. This model fails to converge to provide any solution. Therefore we split the dataset into sites from two geographical areas "Outer Kodiak" and "SE Kodiak"

Model 2: "Outer Kodiak" OxCal model results on page 2, showing the model input in grey, the calibrated age of the radiocarbon sample; in black, the probability density function from Bayesian modelling for each input sample and the 95.4% probability age of the intervening earthquake, labelled "E Kodiak 500". The agreement index [A:] identifies 5 samples that do not agree with the model, where A<60%.

Model 3: "SE Kodiak" OxCal model results on page 3, showing the model input in grey, the calibrated age of the radiocarbon sample; in black, the probability density function from Bayesian modelling for each input sample and the 95.4% probability age of the intervening earthquake, labelled "E Kodiak 200". The agreement index [A:] identifies 3 samples that do not agree with the model, where A<60%.

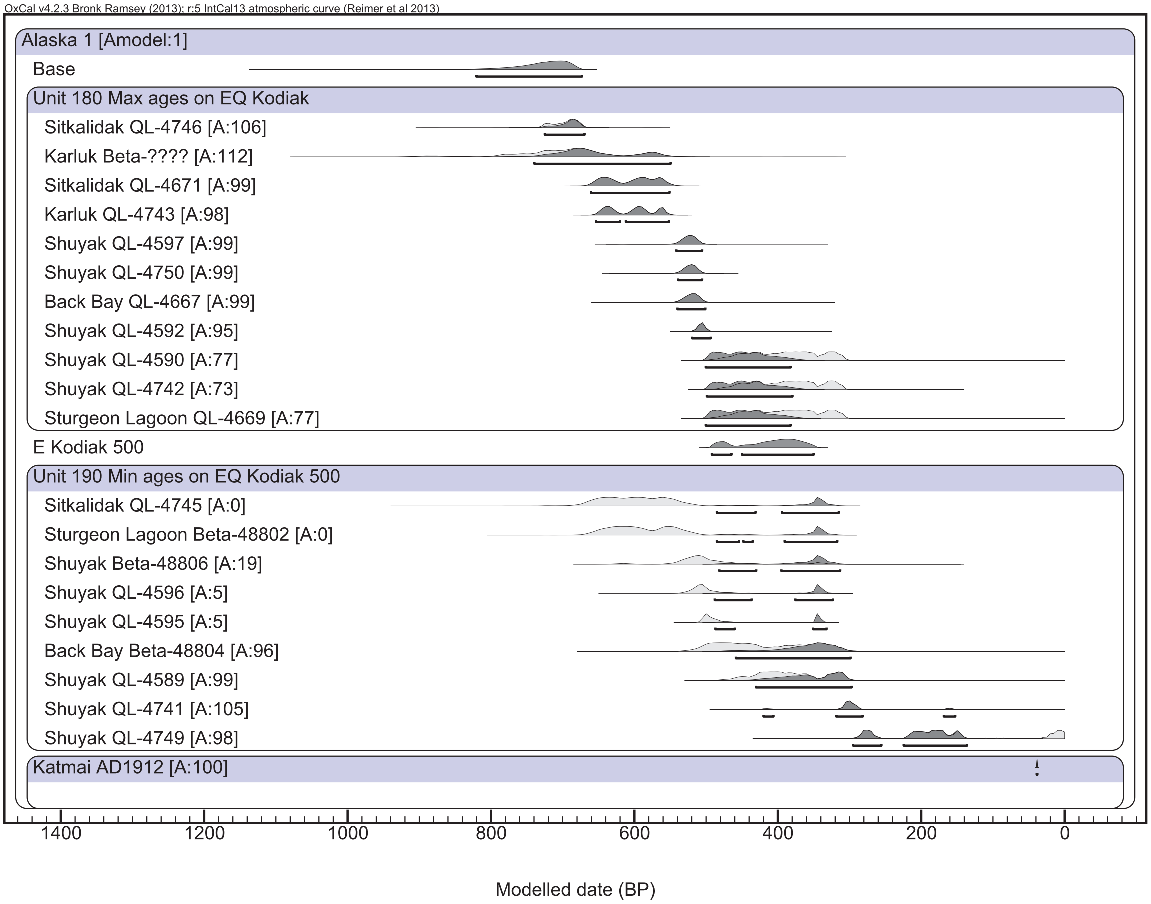
OxCal v4.2.3 Bronk Ramsey (2013); r:5 IntCal13 atmospheric curve (Reimer et al 2013)
Alaska 1 [Amodel:1]
Base
Unit 180 Max ages on EQ Kodiak
Sitkalidak QL-4746 [A:106]
Karluk Beta-???? [A:112]
Sitkalidak QL-4671 [A:99]
Karluk QL-4743 [A:98]
Shuyak QL-4597 [A:99]
Shuyak QL-4750 [A:99]
Back Bay QL-4667 [A:99]
Shuyak QL-4592 [A:95]
Shuyak QL-4590 [A:77]
Shuyak QL-4742 [A:73]
Sturgeon Lagoon QL-4669 [A:77]
E Kodiak 500
Unit 190 Min ages on EQ Kodiak 500
Sitkalidak QL-4745 [A:0]
Sturgeon Lagoon Beta-48802 [A:0]
Shuyak Beta-48806 [A:19]
Shuyak QL-4596 [A:5]
Shuyak QL-4595 [A:5]
Back Bay Beta-48804 [A:96]
Shuyak QL-4589 [A:99]
Shuyak QL-4741 [A:105]
Shuyak QL-4749 [A:98]
Katmai AD1912 [A:100]
1400
1200
1000
800
600
400
200
0
Modelled date (BP)

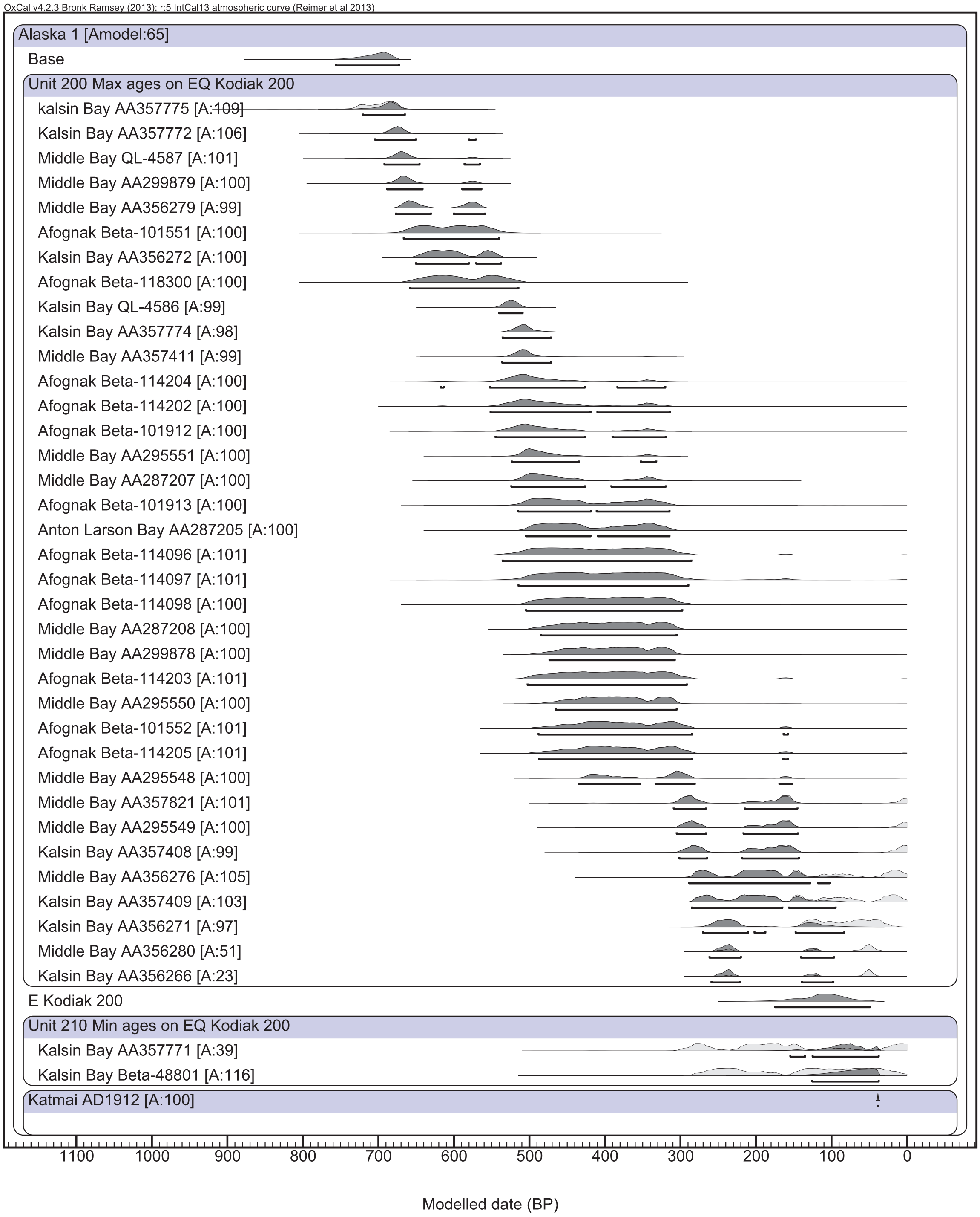

OxCal v4.2.3 Bronk Ramsey (2013); r:5 IntCal13 atmospheric curve (Reimer et al 2013)
Alaska 1 [Amodel:65]
Base
Unit 200 Max ages on EQ Kodiak 200
kalsin Bay AA357775 [A:~~109~~]
Kalsin Bay AA357772 [A:106]
Middle Bay QL-4587 [A:101]
Middle Bay AA299879 [A:100]
Middle Bay AA356279 [A:99]
Afognak Beta-101551 [A:100]
Kalsin Bay AA356272 [A:100]
Afognak Beta-118300 [A:100]
Kalsin Bay QL-4586 [A:99]
Kalsin Bay AA357774 [A:98]
Middle Bay AA357411 [A:99]
Afognak Beta-114204 [A:100]
Afognak Beta-114202 [A:100]
Afognak Beta-101912 [A:100]
Middle Bay AA295551 [A:100]
Middle Bay AA287207 [A:100]
Afognak Beta-101913 [A:100]
Anton Larson Bay AA287205 [A:100]
Afognak Beta-114096 [A:101]
Afognak Beta-114097 [A:101]
Afognak Beta-114098 [A:100]
Middle Bay AA287208 [A:100]
Middle Bay AA299878 [A:100]
Afognak Beta-114203 [A:101]
Middle Bay AA295550 [A:100]
Afognak Beta-101552 [A:101]
Afognak Beta-114205 [A:101]
Middle Bay AA295548 [A:100]
Middle Bay AA357821 [A:101]
Middle Bay AA295549 [A:100]
Kalsin Bay AA357408 [A:99]
Middle Bay AA356276 [A:105]
Kalsin Bay AA357409 [A:103]
Kalsin Bay AA356271 [A:97]
Middle Bay AA356280 [A:51]
Kalsin Bay AA356266 [A:23]
E Kodiak 200
Unit 210 Min ages on EQ Kodiak 200
Kalsin Bay AA357771 [A:39]
Kalsin Bay Beta-48801 [A:116]
Katmai AD1912 [A:100]
1100
1000
900
800
700
600
500
400
300
200
100
0
Modelled date (BP)

Supplemental file - diatom data

Click here to download Supplemental file: Supplementary Information - Diatom assemblage diagrams.pdf

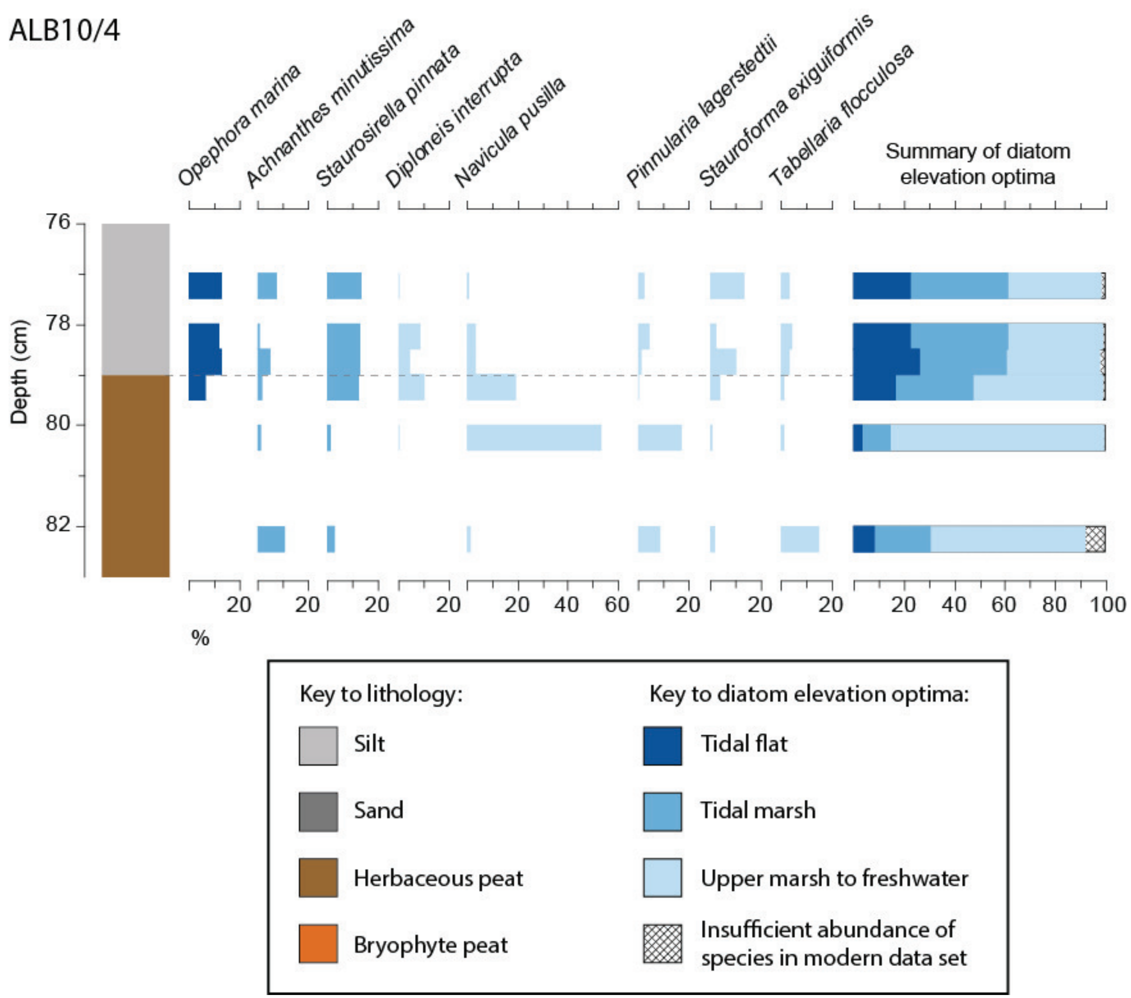

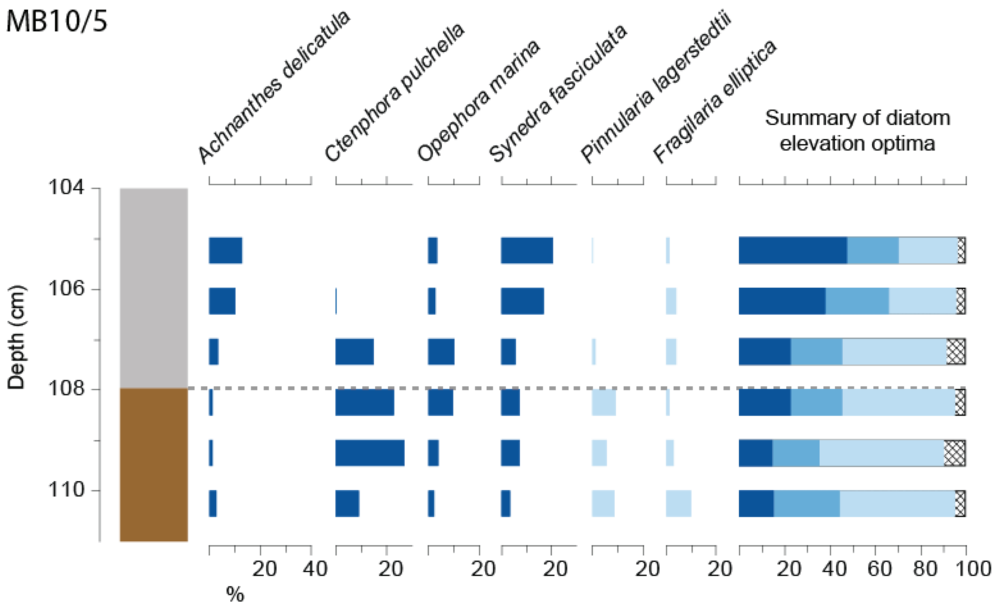
MB10/5
Achnanthes delicatula
Ctenphora pulchella
Opephora marina
Synedra fasciculata
Pinnularia lagerstedtii
Fragilaria elliptica
Summary of diatom elevation optima
Depth (cm)
104
106
108
110
20
40
%
20
20
20
20
20
20
40
60
80
100

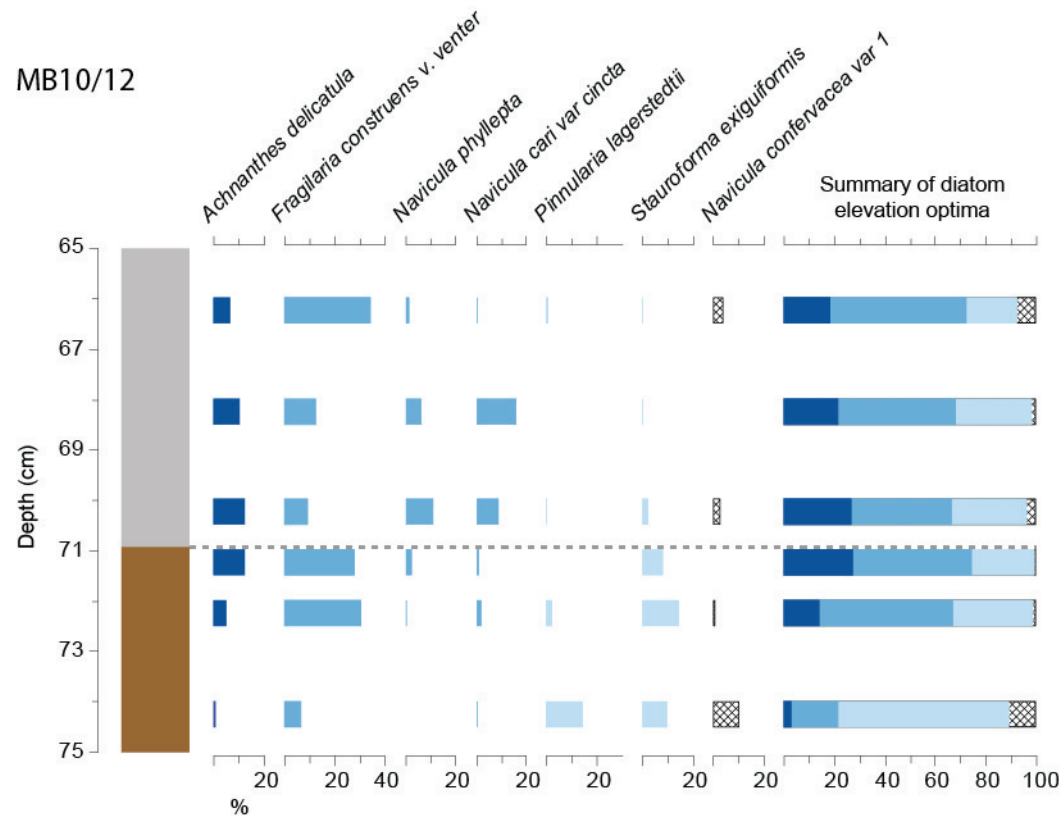
MB10/12
Achnanthes delicatula
Fragilaria construens v. venter
Navicula phyllepta
Navicula cari var cincta
Pinnularia lagerstedtii
Stauroforma exiguiformis
Navicula confervacea var 1
Summary of diatom elevation optima
Depth (cm)
65
67
69
71
73
75
20
20
40
20
20
20
20
20
20
40
60
80
100
%

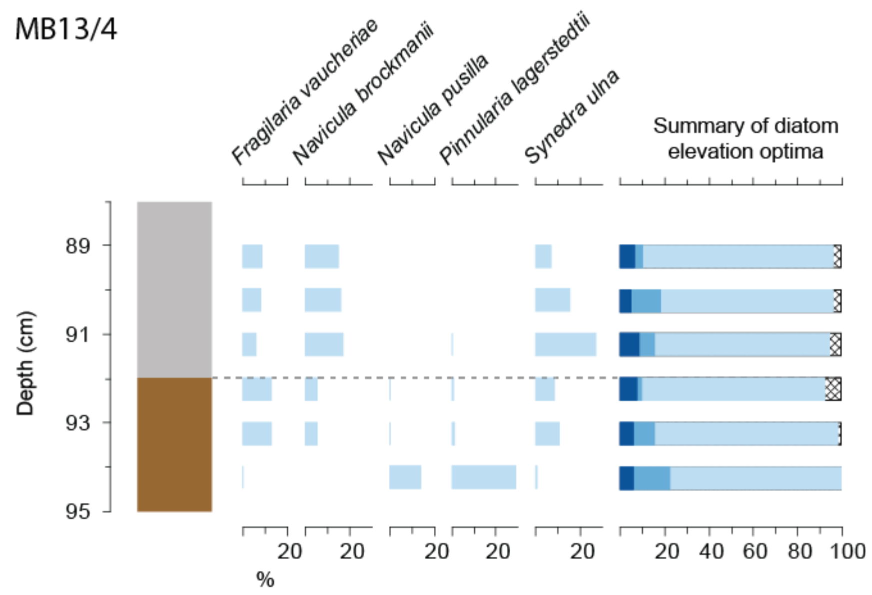
MB13/4
Fragilaria vaucheriae
Navicula brockmanii
Navicula pusilla
Pinnularia lagerstedtii
Synedra ulna
Summary of diatom elevation optima
Depth (cm)
89
91
93
95
20
20
20
20
20
20
40
60
80
100
%

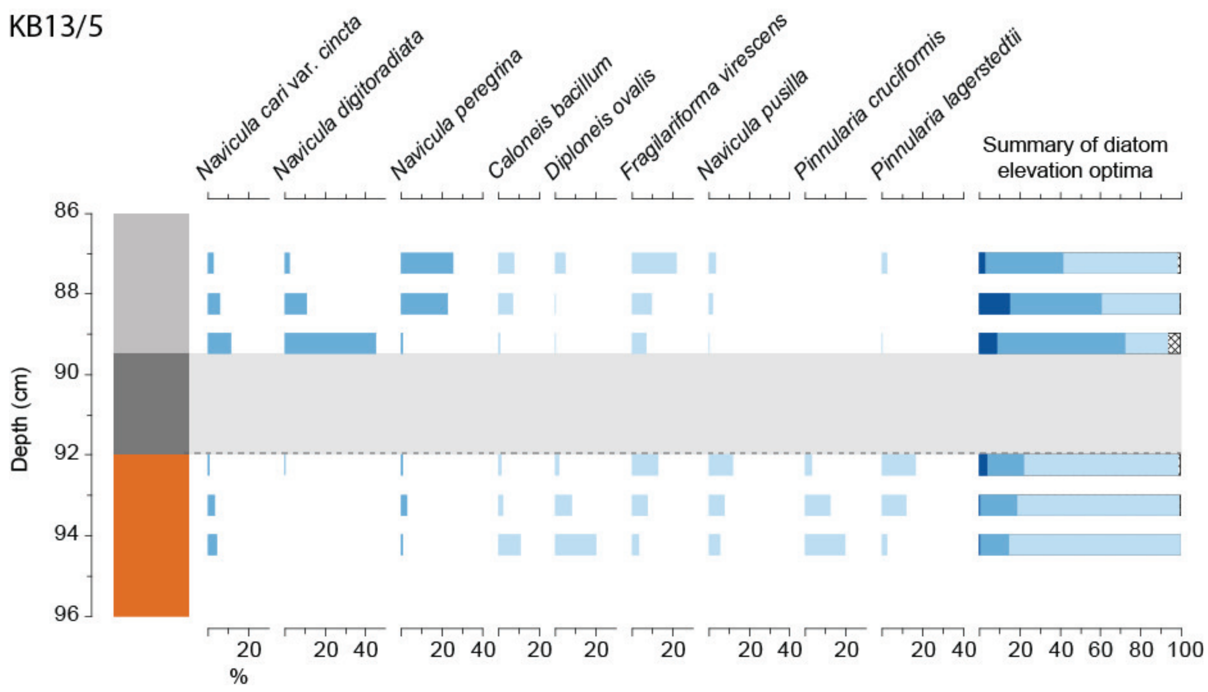
KB13/5
Navicula cari var. cincta
Navicula digitoradiata
Navicula peregrina
Caloneis bacillum
Diploneis ovalis
Fragilariforma virescens
Navicula pusilla
Pinnularia cruciformis
Pinnularia lagerstedtii
Summary of diatom elevation optima
Depth (cm)
86
88
90
92
94
96
20
40
60
80
100
%


KB13/17
Navicula cari var. cincta
Navicula digitoradiata
Navicula peregrina
Caloneis bacillum
Diploneis interrupta
Diploneis ovalis
Fragilariforma virescens
Navicula pusilla
Pinnularia lagerstedtii
Summary of diatom elevation optima
Depth (cm)
92
94
96
98
100
102
104
20
20
20
20
20
20
20 40 60 80
20 40
20
20 40 60 80 100
%

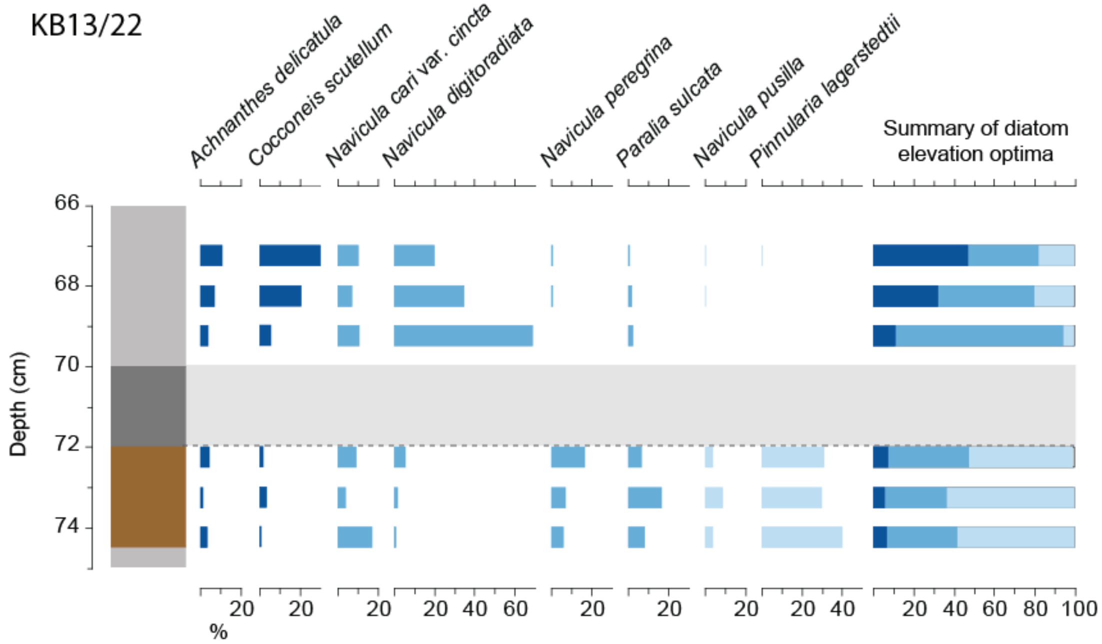
KB13/22
Achnanthes delicatula
Cocconeis scutellum
Navicula cari var. cincta
Navicula digitoradiata
Navicula peregrina
Paralia sulcata
Navicula pusilla
Pinnularia lagerstedtii
Summary of diatom elevation optima
Depth (cm)
66
68
70
72
74
20
40
60
80
100
%

KB13/25

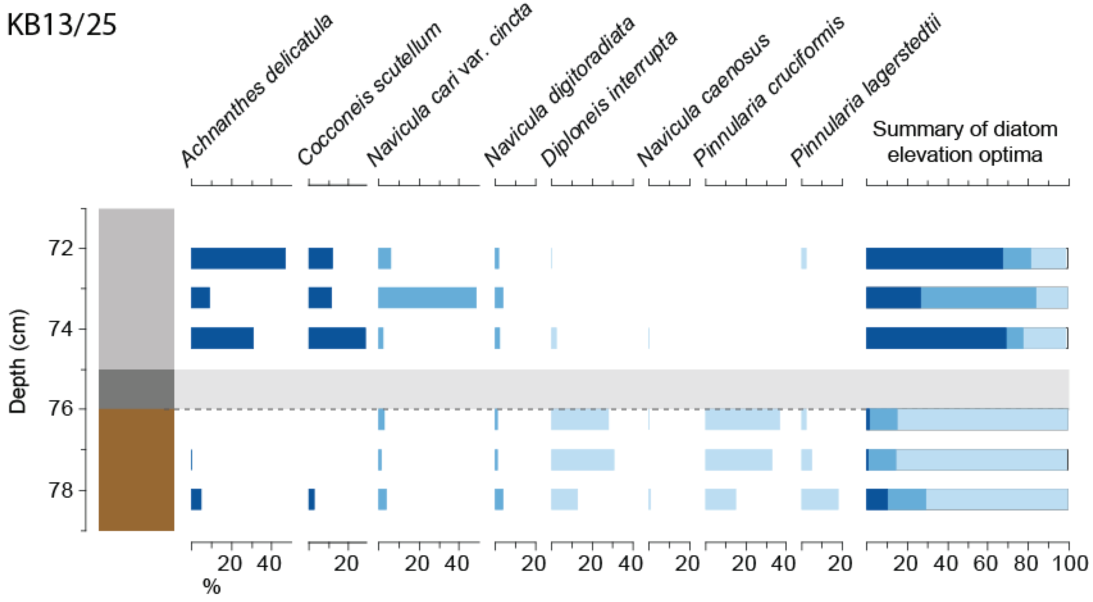

Achnanthes delicatula
Cocconeis scutellum
Navicula cari var. cincta
Navicula digitoradiata
Diploneis interrupta
Navicula caenosus
Pinnularia cruciformis
Pinnularia lagerstedtii
Summary of diatom elevation optima
Depth (cm)
72
74
76
78
20 40
20
20 40
20
20 40
20
20 40
20
20 40 60 80 100
%

KB13/27

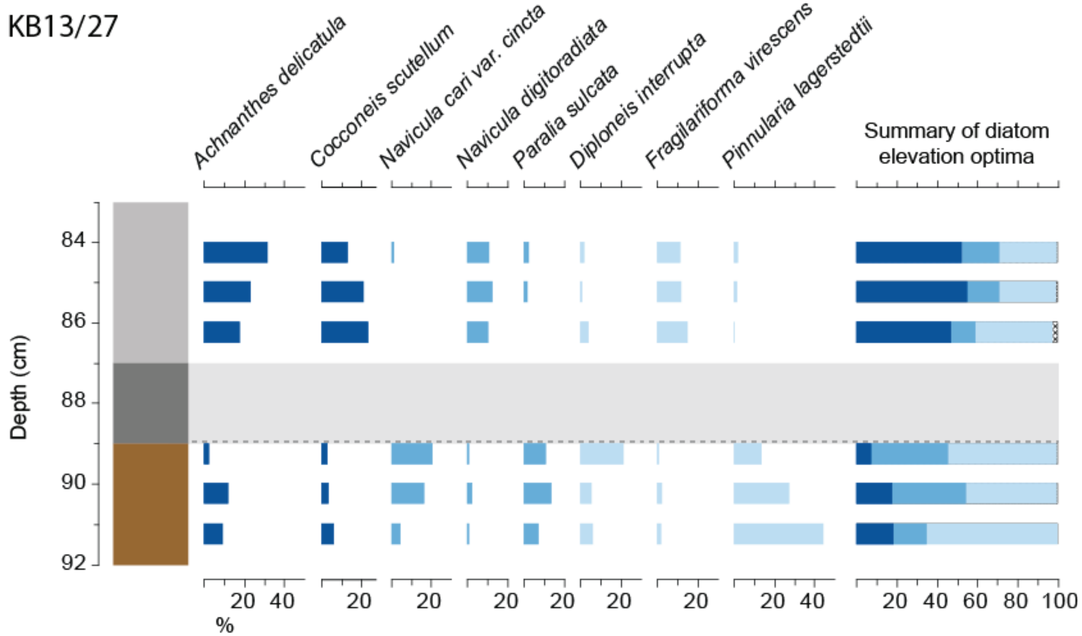

Achnanthes delicatula
Cocconeis scutellum
Navicula cari var. cincta
Navicula digitoradiata
Paralia sulcata
Diploneis interrupta
Fragilariforma virescens
Pinnularia lagerstedtii
Summary of diatom elevation optima
Depth (cm)
84
86
88
90
92
20
40
%
60
80
100

KB13/29

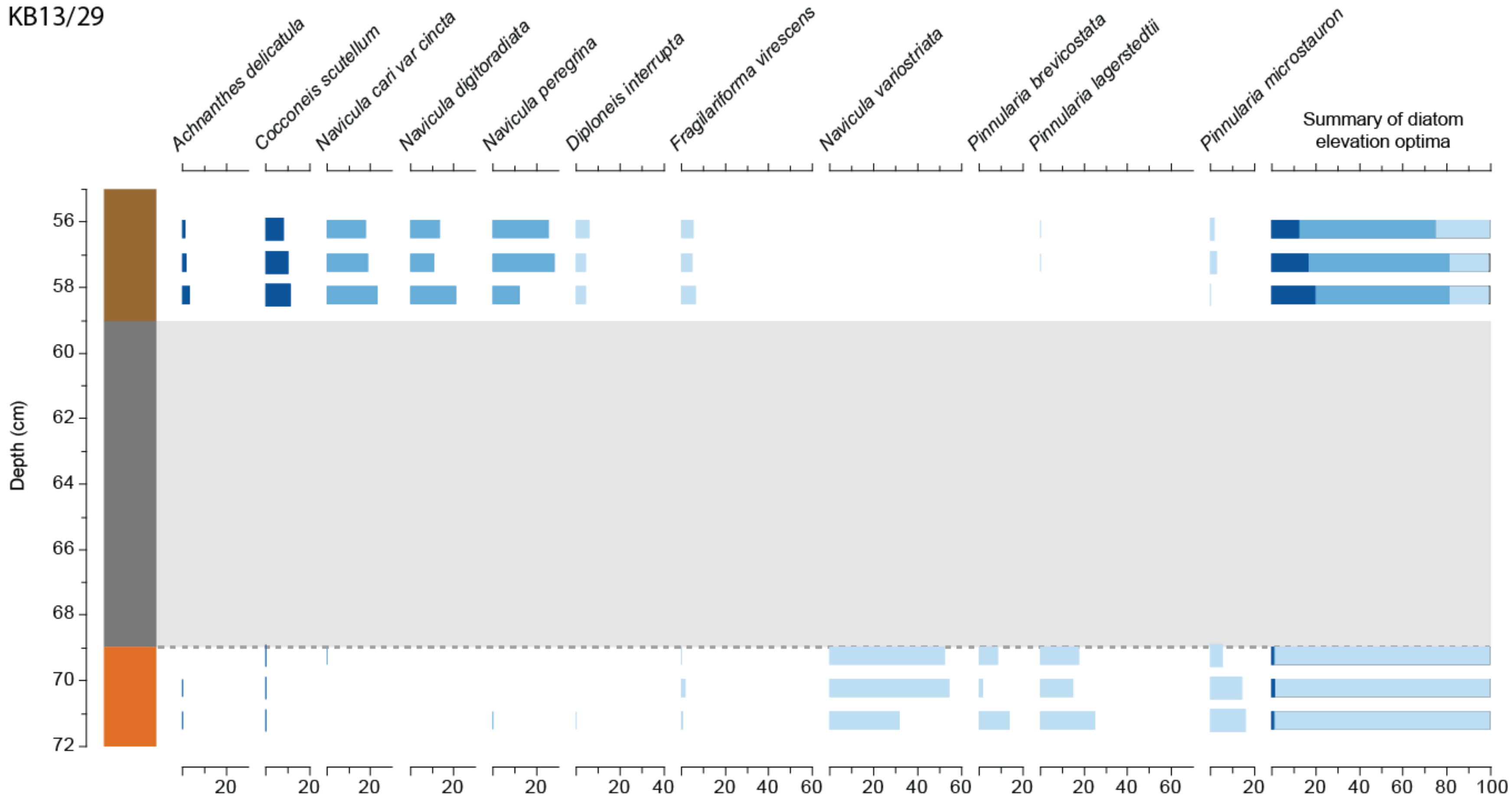

Achnanthes delicatula
Cocconeis scutellum
Navicula cari var cincta
Navicula digitoradiata
Navicula peregrina
Diploneis interrupta
Fragilariforma virescens
Navicula variostriata
Pinnularia brevicostata
Pinnularia lagerstedtii
Pinnularia microstauron
Summary of diatom elevation optima
Depth (cm)
56
58
60
62
64
66
68
70
72
20
40
60
80
100

**Supplementary Information: Diatom-based transfer function reconstructions from separate sample locations**

We use quantitative methods based on transfer function models derived from the distribution of modern diatom assemblages to reconstruct paleo marsh surface elevations for samples from sediment sequences and their diatom assemblages. From these elevation reconstructions we calculate coseismic relative land/sea-level change across an earthquake horizon. Diatom sums are >150 valves and >200 in the majority of cases. We use a modern training set of 206 samples collected from a wide range of marshes across ~1000 km of south central Alaska (Hamilton and Shennan, 2005; Watcham et al., 2013) and from these develop two models to reconstruct elevation. The adoption of which model depends on the lithology of the sediment of each fossil sample (Hamilton and Shennan, 2005); for peat sediment, a model using a subset of 100 modern samples from elevations at which organic sediment or peat was the substrate in the modern sample, and a second for organic silt units and silt units with visible plant rootlets, using all 206 samples. Since none of our fossil samples were from minerogenic units with no visible plant rootlets we did not use the model for those sediments (Hamilton and Shennan, 2005). We assess elevation reconstruction precision using the sample-specific 95.4 % error terms and the goodness of fit between each fossil sample and the modern dataset with a dissimilarity coefficient, using the 20th percentile of the dissimilarity values for the modern samples as the cut-off between 'close' and 'poor' modern analogues for fossil samples. We do not estimate elevation from the diatom assemblages of tsunami deposits due to the high probability of sediment mixing.

Hamilton, S., and Shennan, I., 2005, Late Holocene relative sea-level changes and the earthquake deformation cycle around upper Cook Inlet, Alaska: Quaternary Science Reviews, v. 24, p. 1479-1498.

Watcham, E.P., Shennan, I., and Barlow, N.L.M., 2013, Scale considerations in using diatoms as indicators of sea-level change: lessons from Alaska: Journal of Quaternary Science, v. 28, p. 165-179.

**Supplementary Information: Diatom-based transfer function reconstructions from separate sample locations**

Anton Larson Bay (ALB), Kalsin Bay (KB) and Middle Bay (MB).

Vertical axis: zero = top contact of peat
Gap = tsunami sand, no reconstruction

Transfer function reconstructions
Error bars = 2 SD
White = poor modern analogue
Grey = close modern analogue

KB13-5

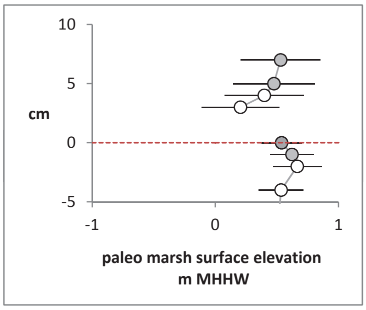


KB13-17

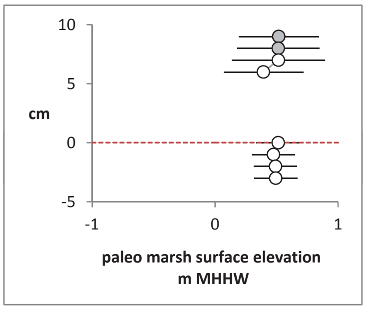


KB 13-25

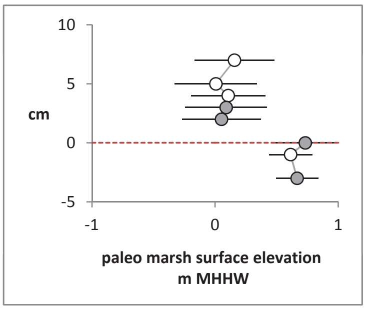


KB 13-22

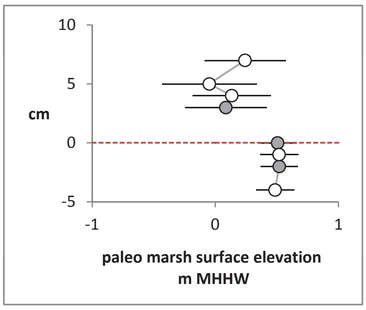


KB 13-29

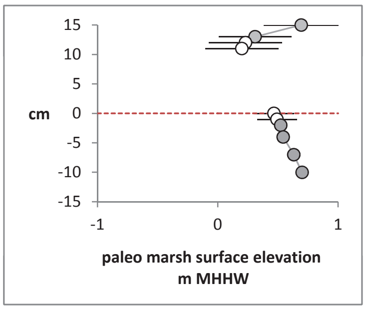


MB 10-5

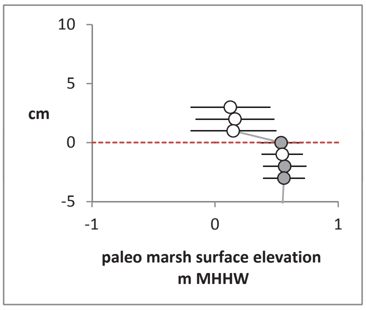


MB 13-1

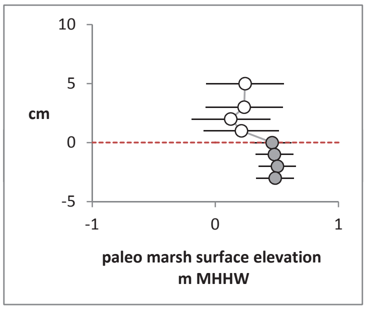


MB 13-4

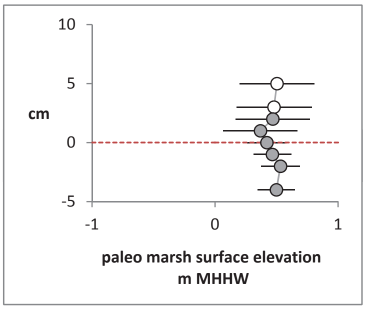


MB 10-12

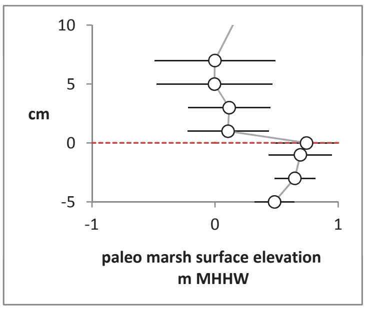


ALB10-4

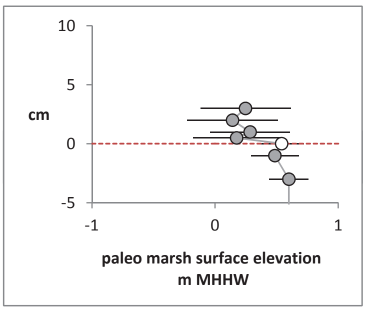

Supplemental file - Kalsin Bay stratigraphy



Kalsin Bay stratigraphy and radiocarbon ages